Alterations in mitosis and cell cycle progression caused by a mutant lamin A known to accelerate human aging

Thomas Dechat*, Takeshi Shimi*, Stephen A. Adam*, Antonio E. Rusinol†, Douglas A. Andres‡, H. Peter Spielmann‡§¶, Michael S. Sinensky†, and Robert D. Goldman*‖

*Department of Cell and Molecular Biology, Feinberg School of Medicine, Northwestern University, 303 East Chicago Avenue, Chicago, IL 60611; †Department of Biochemistry and Molecular Biology, James H. Quillen College of Medicine, East Tennessee State University, Box 70581, Johnson City, TN 37614; and Departments of ‡Molecular and Cellular Biochemistry and §Chemistry and ¶Kentucky Center for Structural Biology, University of Kentucky, 741 South Limestone, Lexington, KY 40536

Communicated by Francis S. Collins, National Institutes of Health, Bethesda, MD, February 2, 2007 (received for review December 19, 2006)

Mutations in the gene encoding nuclear lamin A (LA) cause the premature aging disease Hutchinson–Gilford Progeria Syndrome. The most common of these mutations results in the expression of a mutant LA, with a 50-aa deletion within its C terminus. In this study, we demonstrate that this deletion leads to a stable farnesylation and carboxymethylation of the mutant LA (LAΔ50/progerin). These modifications cause an abnormal association of LAΔ50/progerin with membranes during mitosis, which delays the onset and progression of cytokinesis. Furthermore, we demonstrate that the targeting of nuclear envelope/lamina components into daughter cell nuclei in early G_1 is impaired in cells expressing LAΔ50/progerin. The mutant LA also appears to be responsible for defects in the retinoblastoma protein-mediated transition into S-phase, most likely by inhibiting the hyperphosphorylation of retinoblastoma protein by cyclin D1/cdk4. These results provide insights into the mechanisms responsible for premature aging and also shed light on the role of lamins in the normal process of human aging.

cell division | nuclear lamins | nuclear structure | progeria | protein farnesylation

Hutchinson–Gilford progeria syndrome (HGPS) is an early onset aging disease (1, 2) most commonly caused by a heterozygous mutation in the lamin A (LA) gene (*LMNA*, 1824 C → T) (3, 4). This mutation introduces a splice site, resulting in the expression of a mutant LA (LAΔ50/progerin) (5, 6) that is missing 50 aa near its C terminus. HGPS patients carrying this mutation experience accelerated aging symptoms, including loss of s.c. fat, growth retardation, hair loss, skeletal hypoplasia and dysplasia, osteoporosis, and arteriosclerosis. Patients usually die at an average of 15 years of age from heart attacks or strokes (7). Other than HGPS, various diseases, including muscular dystrophies and lipodystrophies, have been linked to mutations in *LMNA* (8).

Lamins are intermediate filament proteins located in the nuclear lamina and throughout the nucleoplasm (9, 10). In humans, lamins are divided into A and B types. The major A-type lamins, LA and lamin C (LC), are derived from a single gene by alternative splicing, whereas B-type lamins (LB) are encoded by different genes. Lamins A and B are modified at their C-terminal −CAAX box in a series of steps involving farnesylation of the cysteine residue, cleavage of −AAX, and carboxymethylation (11, 12). Whereas LB is permanently farnesylated/carboxymethylated, LA is cleaved by Zmpste24, a zinc-metalloproteinase, removing another 15 aa from the C terminus, including the farnesylated/carboxymethylated cysteine (13–15). Because the cleavage site for Zmpste24 is missing in LAΔ50/progerin, it is thought, but has yet to be demonstrated biochemically, that it is stably farnesylated (16).

In interphase cells, the expression of LAΔ50/progerin leads to nuclear lobulation, thickening of the lamina, genome instability, DNA repair defects, changes in histone methylation, and loss of heterochromatin (5, 17–19). However, the impact of LAΔ50/progerin on mitosis and its consequences for daughter cells entering G_1 have not been determined. An initial insight into changes in early G_1 came from studies of HeLa cells expressing GFP-LAΔ50/progerin, in which this mutant protein is abnormally retained in cytoplasmic structures after nuclear assembly is completed (5). Here, we provide further insights into the composition of these structures and the impact of LAΔ50/progerin on cell division, nuclear assembly, and the cell cycle.

Results

First, we verified that cytoplasmic structures similar to those seen in GFP-LAΔ50/progerin transfected HeLa cells (5) were present in HGPS patient fibroblasts. We found that daughter cells in early G_1 contained abnormal cytoplasmic structures enriched in LA/C (Fig. 1 *Aa*, *Ad*, and *Ag*). These structures also react with anti-LA (Fig. 1 *Aa–Ac*), which does not crossreact with LAΔ50/progerin [supporting information (SI) Fig. 6], and with anti-LB and anti-emerin, an integral nuclear membrane protein known to bind to LA (20) (Fig. 1 *Ad–Ai*). In control fibroblasts, LA/C, LB, and emerin are sequestered in the nucleus in early G_1 as expected (data not shown). These observations suggest that LAΔ50/progerin causes the aberrant retention of nuclear membrane and lamina components in the cytoplasm well into G_1. At times after cell division (e.g., late G_1, S), all detectable LAΔ50/progerin, LA/C, LB, and emerin are located in the nucleus (data not shown and ref. 5).

The retention of nuclear components in the cytoplasm in early G_1 in HGPS fibroblasts suggests that progression through the cell cycle is altered, which could affect the G_1/S transition (5). To test this possibility, we examined the retinoblastoma protein (Rb) in HGPS cell nuclei, because it binds to LA (21) and its hyperphosphorylated form (phosphoRb) is required for the G_1/S transition (22). In the majority (94.2%, $n = 53$) of HGPS cells with highly lobulated nuclei and a thickened lamina (Fig. 1 *Ba–Bc*, red) (5), we could not detect phosphoRb by using an antibody against the phosphorylated Rb

Author contributions: T.D., T.S., A.E.R., M.S.S., and R.D.G. designed research; T.D., T.S., A.E.R., and M.S.S. performed research; S.A.A., D.A.A., and H.P.S. contributed new reagents/analytic tools; T.D., T.S., A.E.R., M.S.S., and R.D.G. analyzed data; and T.D., A.E.R., M.S.S., and R.D.G. wrote the paper.

The authors declare no conflict of interest.

Abbreviations: AG, anilinogeraniol; FTase, farnesyl transferase; FTI, FTase inhibitor; HGPS, Hutchinson–Gilford progeria syndrome; LA, lamin A; LB, B-type lamins; LC, lamin C; LAΔ50/progerin, mutant LA in HGPS cells; NEBD, nuclear envelope breakdown; Rb, retinoblastoma protein.

‖To whom correspondence should be addressed. E-mail: r-goldman@northwestern.edu.

This article contains supporting information online at www.pnas.org/cgi/content/full/0700854104/DC1.

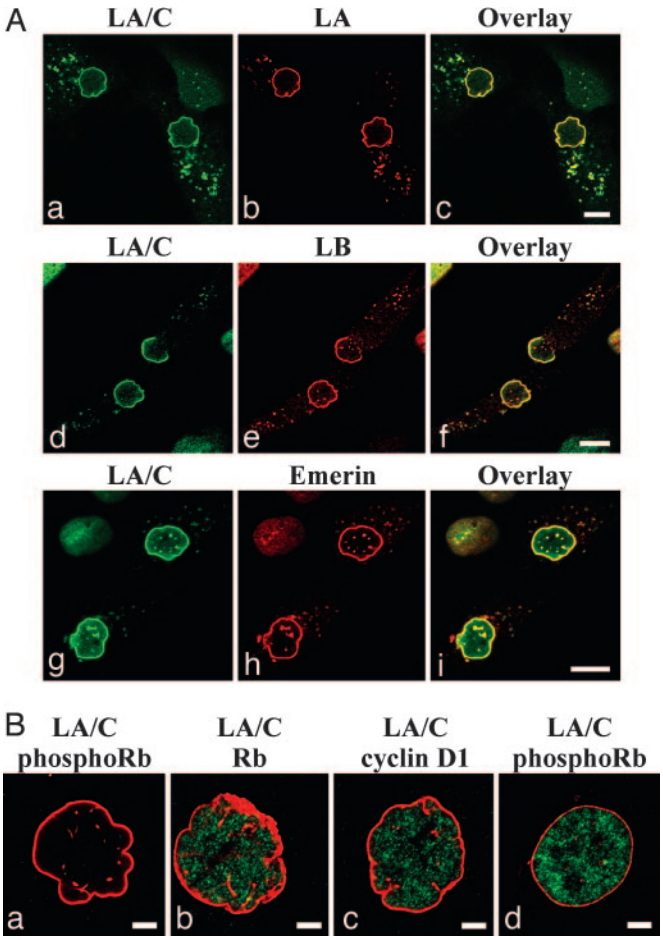

Fig. 1. Cells from HGPS patients expressing LAΔ50/progerin contain abnormal cytoplasmic structures enriched in nuclear lamina/envelope components in early G_1. (*A*) Mid- to late-passage (p) (5) HGPS fibroblasts (HGADFN003, p18) were fixed in 3% paraformaldehyde and processed for immunofluorescence with anti-LA/C (*a*, *d*, and *g*), anti-LA (*b*), anti-LB (*e*), and anti-emerin (*h*). Early G_1 cells displayed abnormal cytoplasmic structures containing LA/C (*a*, *c*, *d*, *f*, *g*, and *i*), LA (*b* and *c*), LB (e and *f*), and emerin (*h* and *i*). These structures are also seen in HGPS fibroblasts from another patient (HGADFN127, p16) but not in control fibroblasts [AG08470 (p17) and AG09309 (p18)] (data not shown). Confocal images are shown. (Scale bars, 10 μm.) (*B*) Late passage HGPS fibroblasts (HGADFN003, p22) were methanol fixed and processed for double immunofluorescence by using anti-LA/C (*a–d*, red) and either anti-phosphoRb-(Ser-807/811) (*a* and *d*, green), anti-Rb (*b*, green), or anti-cyclin D1 (*c*, green). Confocal images are shown. (Scale bars, 5 μm.)

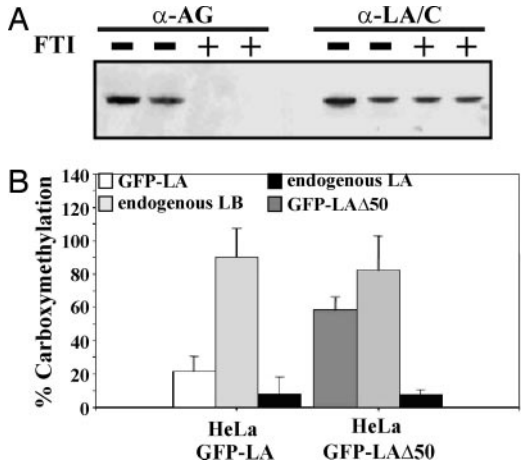

Fig. 2. LAΔ50/progerin is farnesylated and carboxymethylated. (*A*) HeLa cells expressing GFP-LAΔ50/progerin were incubated with the farnesol analogue, AG, and with (+FTI) or without (−FTI) 3 μM FTI-277. GFP-LAΔ50/progerin was immunoprecipitated with anti-GFP and analyzed by immunoblotting, using either anti-AG (α-AG) or anti-LA/C (α-LA/C). The results of two experiments (±FTI) are shown. (*B*) HeLa cells expressing GFP-LAΔ50/progerin or GFP-LA were incubated with ([*methyl*-^{3}H])methionine for 16–20 h. After incubation, proteins were immunoprecipitated consecutively with antibodies against LB, LA, and EGFP, separated on SDS/PAGE, and identified by immunoblotting. Protein bands (n = 3) were excised, and carboxymethylation was determined as described in *Materials and Methods*.

residues Ser-807/811 (Fig. 1*Ba*, green). Patients' cells with normally shaped nuclei and a typical lamina frequently (38.5%, n = 53) contained phosphoRb (Fig. 1*Bd*, green), indicating that they are in either S or G_2/M (22). However, Rb was present in the highly lobulated nuclei (Fig. 1*Bb*, green), suggesting that the absence of phosphoRb is not due to degradation. Cyclin D1, a cofactor for cdk 4 that phosphorylates Rb at Ser-807/811 (23), is present in the lobulated nuclei (Fig. 1*Bc*, green). This suggests that LAΔ50/progerin impairs the Rb-mediated G_1/S transition because of inhibition of cdk4 activity.

To gain insights into the mechanisms responsible for the formation of the abnormal cytoplasmic nuclear membrane/lamina components, we determined whether LAΔ50/progerin is farnesylated. This posttranslational modification might cause an abnormal affinity for membranes (11, 24). Previously, mass-spectrometry was used to detect CAAX box modifications on gel purified pre-LA (14). Because we have encountered technical difficulties applying this approach to LAΔ50/progerin, we have used an alternative assay developed to detect the farnesylation of a CAAX protein (25). In this assay, a farnesol analogue, 8-anilinogeraniol (AG), is used as a prosubstrate for the farnesyl transferase (FTase). Detection of the unnatural lipid is achieved by immunoblotting with anti-AG. An important control to verify that an FTase is mediating incorporation of AG is inhibition with the FTase inhibitor (FTI), FTI-277. By using this approach, GFP-LAΔ50/progerin was immunoprecipitated from HeLa cells incubated with 8-AG and analyzed by immunoblotting (Fig. 2*A*). In the absence of the FTI (FTI−), a band of the expected molecular weight was detected with anti-AG (α-AG) and anti-LA/C (α-LA/C). However, when cells were treated with FTI-277 before immunoprecipitation (FTI+), only α-LA/C showed immunoreactivity. These results demonstrate that LAΔ50/progerin is farnesylated.

Verification of carboxymethylation of LAΔ50/progerin was obtained by means of a base-release assay (12), which also provides a relative measure of the amount of LAΔ50/progerin that is completely processed at the −CAAX box. For this purpose, HeLa cells expressing GFP-LAΔ50/progerin or GFP-LA were incubated with ([*methyl*-^{3}H])methionine and used for immunoprecipitation of endogenous LA, LB, GFP-LA, and GFP-LAΔ50/progerin. The immunoprecipitated proteins were further analyzed (see *Materials and Methods*). The results of these experiments show that GFP-LAΔ50/progerin is carboxymethylated to about the same extent as LB, whereas endogenous LA and GFP-LA are not carboxymethylated (Fig. 2*B*).

To determine the effects of the permanent state of farnesylation of LAΔ50/progerin, GFP-LAΔ50/progerin expression was studied in HeLa cells. During interphase, GFP-LAΔ50/progerin could not be detected in the nucleoplasm (SI Fig. 7). Rather, it localized exclusively to the nuclear lamina region, most likely anchored to the inner nuclear membrane because of farnesylation (11, 16, 24). In contrast, GFP-LA was also present as a nucleoplasmic veil in interphase nuclei (SI Fig. 7). We also determined the impact of the membrane association of LAΔ50/progerin during mitosis. In normal cells, lamin depolymerization

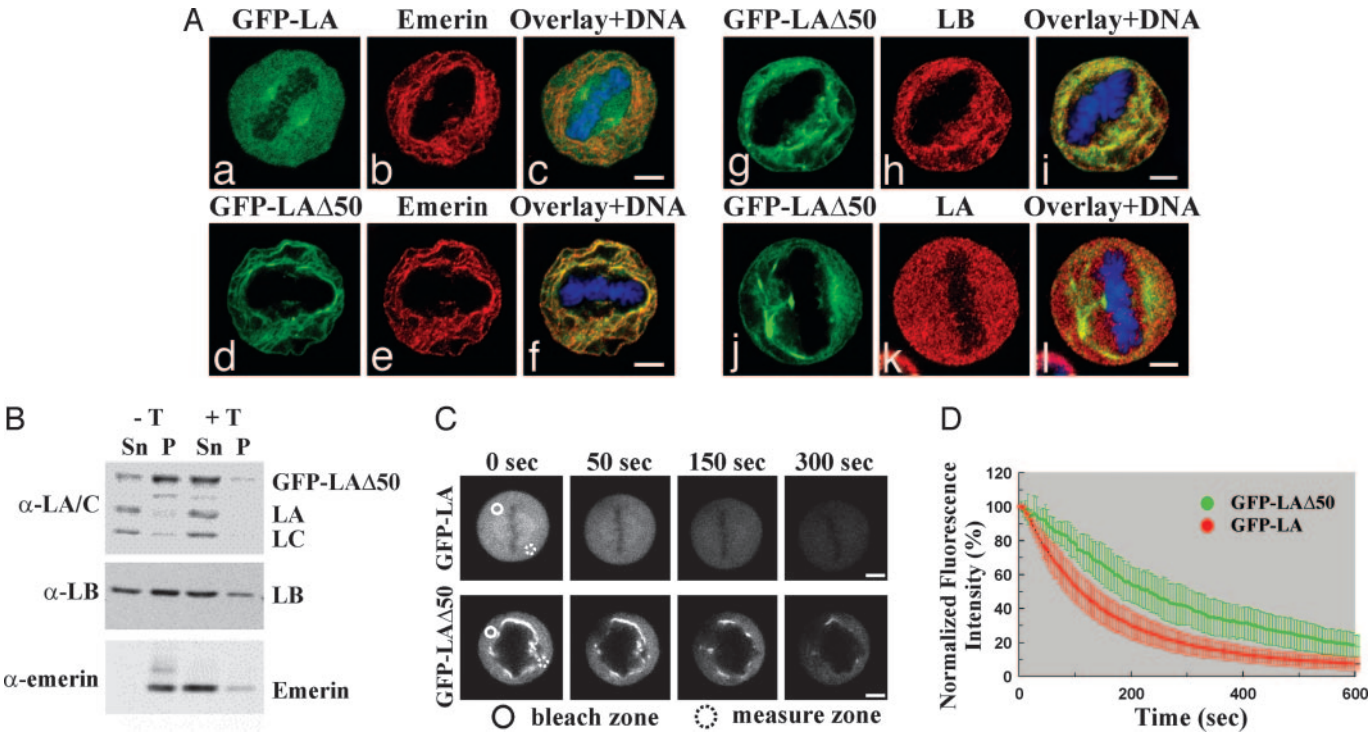

Fig. 3. LAΔ50/progerin is membrane associated during mitosis. (*A*) HeLa Tet-on cells expressing either GFP-LA (*a–c*) or GFP-LAΔ50/progerin (*d–l*) were fixed with 3.7% formaldehyde and processed for immunofluorescence by using anti-emerin (*b*, *c*, *e*, and *f*), anti-LA (*k* and *l*), and anti-LB (*h* and *i*). DNA was stained with Hoechst dye (*c*, *f*, *i*, and *l*). Confocal images of metaphase cells are shown. (Scale bars, 5 μm.) (*B*) HeLa Tet-on cells expressing GFP-LAΔ50/progerin were arrested in mitosis and extracted with (+T) or without (−T) detergent (see *Materials and Methods*). Supernatant (Sn) and pellet (P) fractions were collected. Immunoblots using anti-LA/C (α-LA/C), anti-LB (α-LB), or anti-emerin (α-emerin) are shown. (*C* and *D*) Fluorescence loss in photobleaching analyses of metaphase HeLa Tet-on cells expressing either GFP-LA or GFP-LAΔ50/progerin. GFP-fluorescence was repeatedly photobleached in the area indicated by the closed white circle at ≈4-sec intervals. An image was captured immediately after each time interval. (*C*) Images of representative time points are shown (0 sec represents prephotobleach). The fluorescence intensity was measured at each time point in an area opposite to the photobleached area (dotted white circle). (Scale bars, 5 μm.) (*D*) The images obtained from 10 GFP-LA (red dots) and from 11 GFP-LAΔ50/progerin (green dots) expressing metaphase cells were analyzed (see *SI Materials and Methods*). For each time point, the normalized fluorescence intensity measurements were averaged and plotted as a function of time. Error bars are indicated for each time point.

takes place during nuclear envelope breakdown (NEBD) (10, 26). Whereas depolymerized LA/C is dispersed throughout the cytoplasm in metaphase, LB remains mainly membrane associated (26). Studies of mitotic HeLa cells expressing either GFP-LA or GFP-LAΔ50/progerin revealed that GFP-LAΔ50/progerin colocalized with emerin and LB in membranous structures in metaphase (Fig. 3 *Ad–Ai*), but not with endogenous LA (Fig. 3 *Aj–Al*). Similar structures are also detected in metaphase HGPS cells with a specific LAΔ50/progerin antibody [see accompanying paper by Cao *et al.* (27)]. As expected, GFP-LA was uniformly distributed throughout the cytoplasm, sparing only the chromosomes, and it did not colocalize with emerin or LB (Fig. 3 *Aa–Ac* and data not shown). In addition, GFP-LA appeared to be more concentrated in the metaphase spindle in close proximity to microtubules (SI Fig. 8), whereas GFP-LAΔ50/progerin appeared to be greatly reduced in this region (SI Fig. 8). Upon the addition of FTI-277, the association of GFP-LAΔ50/progerin with membranes was no longer detectable in mitotic cells (SI Fig. 8). Rather, it appeared to be uniformly distributed and indistinguishable from GFP-LA in metaphase cells. Under these conditions, LAΔ50/progerin also appeared to be more concentrated in metaphase spindles as was the case for GFP-LA (SI Fig. 8). These data are especially interesting, because it has recently been shown that lamins are required for the formation of the mitotic spindle matrix (28).

Other evidence supporting the association of LAΔ50/progerin with membranes during mitosis was derived from biochemical fractionation studies. Mitotically arrested HeLa cells expressing GFP-LAΔ50/progerin were lysed, and supernatant (Sn) and pellet (P) fractions were collected in the presence or absence of Triton X-100 (see *Materials and Methods*). Analysis of these fractions by immunoblotting revealed that, in the absence of detergent, the vast majority of GFP-LAΔ50/progerin, LB, and emerin were in the insoluble pellet (Fig. 3*B*, −T). In contrast, most LA/C was in the soluble supernatant (Fig. 3*B*, −T). Upon the addition of Triton X-100, there was a shift of GFP-LAΔ50/progerin, LB and emerin to the soluble fraction (Fig. 3*B*, +T). In control cells expressing GFP-LA, almost all GFP-LA and LA/C remained in the soluble fraction under both conditions (data not shown). These results further demonstrate that LAΔ50/progerin is abnormally attached to membranes during mitosis.

We also determined whether the process of GFP-LAΔ50/progerin disassembly during NEBD differed from that of GFP-LA, using live imaging of HeLa cells. In control cells, GFP-LA was located in the nuclear periphery and the nucleoplasm during the early stages of NEBD. As NEBD progressed, GFP-LA became uniformly distributed throughout the cytoplasm (SI Movie 1). In contrast, GFP-LAΔ50/progerin was not detected within the nucleoplasm in cells at any time during NEBD. Rather, it was redistributed from the nuclear periphery to cytoplasmic membrane structures (SI Movie 2).

We next compared the dynamic properties of GFP-LAΔ50/progerin with GFP-LA during metaphase in HeLa cells, using fluorescence loss in photobleaching assays. These assays demonstrated that the GFP-LA signal decreased uniformly throughout the entire cell (Fig. 3*C Upper*), whereas the GFP-LAΔ50/progerin signal was lost in a more gradual fashion away from the bleach zone (Fig. 3*C Lower*). The time for loss of ≈50%

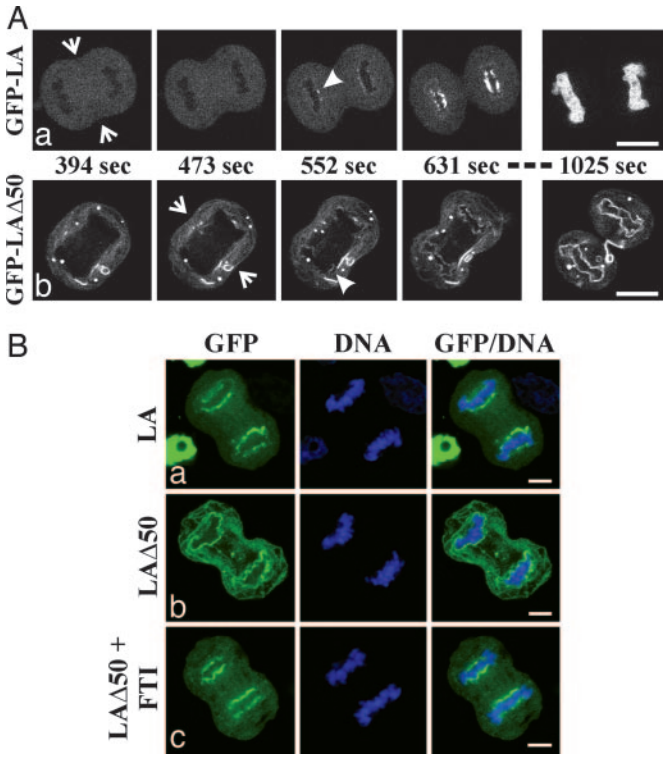

Fig. 4. LAΔ50/progerin re-localizes exclusively to the nuclear periphery at the end of mitosis and delays cytokinesis and nuclear envelope reassembly. (*A*) HeLa Tet-on cells expressing either GFP-LA (*a*) or GFP-LAΔ50/progerin (*b*) were followed by time-lapse microscopy from the metaphase/anaphase transition (0 sec) into G_1. Confocal images were acquired at ≈79-sec intervals (see *SI Materials and Methods*). Representative time points for the onset of cytokinesis (arrows) and for the initial localization of the GFP-fusion proteins to the newly forming sister nuclei (arrowheads) are shown (394–631 sec), as well as the time when most of the GFP-LA was located in the nucleus (1,025 sec). (Scale bars, 10 μm.) (*B*) GFP-LA- (*a*) and GFP-LAΔ50/progerin- (*b*) expressing HeLa Tet-on cells were fixed with 3.7% formaldehyde, and DNA was stained with Hoechst dye. In addition, GFP-LAΔ50/progerin expressing cells were incubated with FTI-277 before fixation (*c*). Confocal images of telophase cells are shown. (Scale bars, 5 μm.)

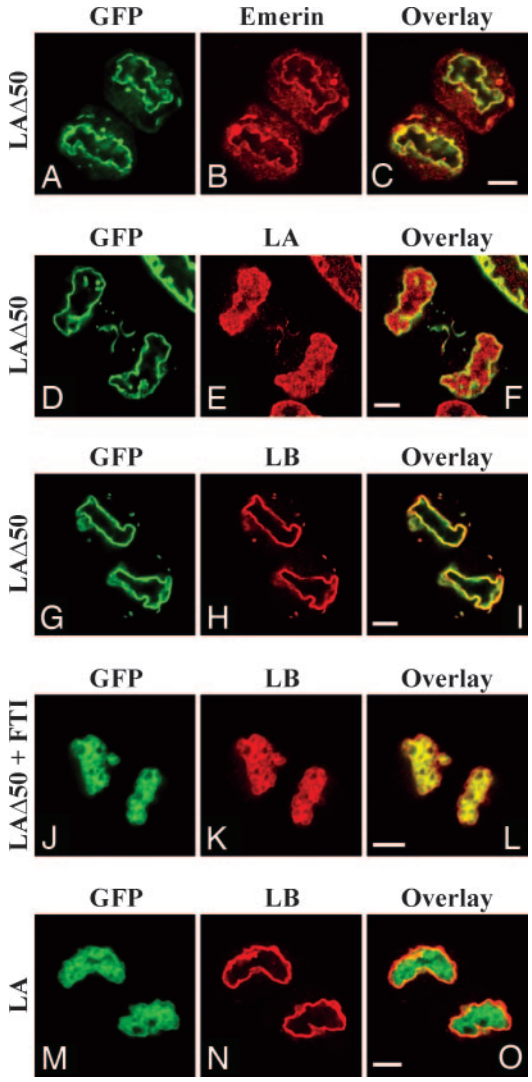

Fig. 5. LA and LB are retained in the cytoplasm in early G_1 cells expressing GFP-LAΔ50/progerin. HeLa Tet-on cells expressing either GFP-LAΔ50/progerin (*A–I*) or GFP-LA (*M–O*) were fixed with 3.7% formaldehyde and processed for immunofluorescence by using anti-emerin (*B* and *C*), anti-LA (*E* and *F*) and anti-LB (*H*, *I*, *K*, *L*, *N*, and *O*). In addition, GFP-LAΔ50/progerin expressing cells were incubated with FTI-277 before fixation (*J–L*). Confocal images of late telophase/early G_1 cells are shown. (Scale bars, 5 μm.)

GFP-LAΔ50/progerin fluorescence was ≈232 sec, compared with ≈111 sec for GFP-LA (Fig. 3*D*). These results suggest that the mobility of GFP-LAΔ50/progerin is constrained because of its association with membranes, whereas GFP-LA can freely diffuse throughout the cytoplasm.

To determine whether the attachment of LAΔ50/progerin to membranes during mitosis leads to mitotic defects that could contribute to the phenotype seen in HGPS fibroblasts in early G_1, time-lapse studies beginning with the metaphase/anaphase transition until late cytokinesis were carried out on live HeLa cells expressing GFP-LA ($n = 9$) or GFP-LAΔ50/progerin ($n = 8$). First, we determined the time taken from the metaphase/anaphase transition to the initiation of the cleavage furrow, which represents the onset of cytokinesis (see arrows in Fig. 4*A*). The average time in GFP-LA-expressing cells was 412 ± 35 sec, and in cells expressing GFP-LAΔ50/progerin it was 483 ± 51 sec, to the initiation of cleavage (Fig. 4*A* and SI Movies 3 and 4). This finding reflects a delay of ≈17% ($P = 0.0039$) in the time of onset of cytokinesis in cells expressing GFP-LAΔ50/progerin. Next, we determined the timing of the relocalization of both the mutant and wild type proteins to segregating sister chromatids. The two proteins did not show significant differences in the timing of their initial relocalization [543 ± 26 sec for GFP-LA vs. 522 ± 41 sec for GFP-LAΔ50/progerin ($P = 0.2205$); see arrowheads in Fig. 4*A*]. However, GFP-LAΔ50/progerin relocated to and remained exclusively at the periphery of segregating sister chromatids (Fig. 4 *Ab* and *Bb* and SI Movie 4), a pattern similar to that seen for LB (29); whereas GFP-LA relocalized initially to the "core regions" of sister chromatids (29) and subsequently accumulated throughout the forming nucleoplasm (Figs. 4 *Aa* and *Ba* and 5*m*, and SI Movie 3). The addition of FTI-277 to GFP-LAΔ50/progerin-expressing cells caused a reversion to patterns seen in GFP-LA-expressing cells (Figs. 4 *Bc* and 5*J*).

Regarding the timing of the completion of nuclear relocalization, GFP-LAΔ50/progerin was retained in the cytoplasm in late telophase/early G_1 compared with GFP-LA, which was similar to the observations made in HGPS cells. In cells expressing GFP-LA, it took 1,060 ± 42 sec from the metaphase/anaphase transition until all detectable GFP-LA was located in the newly formed nuclei (Fig. 4 *Aa*, 1,025 sec). However, at this same time point there was still a significant amount of GFP-LAΔ50/progerin present in the cytoplasm (Fig. 4*Ab*, 1,025 sec). This was true for all cells expressing GFP-LAΔ50/progerin, even after

≈2,100 sec of observation from the metaphase/anaphase transition (SI Movie 4 and data not shown).

We also determined the extent of similarity of the cytoplasmic structures containing GFP-LAΔ50/progerin found in HeLa cells in early G_1 with those seen in HGPS cells. In this regard, we found that endogenous LA, LB, and emerin colocalized with GFP-LAΔ50/progerin in similar cytoplasmic structures (Fig. 5 *A–I*). Upon treatment with FTI-277, GFP-LAΔ50/progerin was no longer detectable in the cytoplasm in late telophase/early G_1 cells (Fig. 5*J*). Rather, it was distributed throughout the nucleoplasm, instead of being concentrated in the lamina region, as was the case for farnesylated GFP-LAΔ50/progerin. The distribution of LB is also altered from its normal association with the surface of daughter cell nuclei to a nucleoplasmic pattern in FTI-277-treated cells (compare Fig. 5 *N* and *K*), colocalizing with GFP-LAΔ50/progerin (Fig. 5*L*). This may be relevant, because plans for treating HGPS patients with FTIs are now under consideration. Cytoplasmic structures containing LA and LB were not detected in either GFP-LAΔ50/progerin-expressing cells treated with FTI-277 or GFP-LA-expressing cells in late telophase/early G_1 (Fig. 5 *J–O* and data not shown).

Discussion

The results of this study demonstrate that LAΔ50/progerin is stably farnesylated/carboxymethylated and that this leads to its abnormal association with membranes during mitosis. This defect delays the onset and progression of cytokinesis and the targeting of nuclear envelope components to daughter cell nuclei in late telophase/early G_1. A delay in the progression through cytokinesis supports the finding by Cao *et al.* (see accompanying paper) that HeLa cells expressing GFP-LAΔ50/progerin have an increased mitotic index, compared with those expressing GFP-LA. These delays undoubtedly have a negative impact on the spatially and temporally regulated sequence of events that represent the hallmarks of normal cell cycle progression. In support of this hypothesis, we provide evidence that the Rb-mediated progression into S-phase is impaired in HGPS cells.

One possible link between LAΔ50/progerin expression and a decrease of Rb hyperphosphorylation may be INK4a, an inhibitor of cyclin D-dependent kinase activity (30). In support of this possibility, it has been shown that LA/C is required for INK4a-mediated G_1 arrest and that LAΔ50/progerin can restore INK4a responsiveness in $LMNA^{-/-}$ cells (31). Interestingly, INK4a is also thought to play a role in the aging process, possibly through reduction of the replicative potential of adult stem cells (30). This finding is of special interest, as recently it has been suggested that impaired adult stem cell function and tissue regeneration may be responsible for diseases caused by the numerous mutations in *LMNA* (32).

In contrast to $ZMPSTE24^{-/-}$ mice, in which decreased Rb levels have been described (33), Rb was still present in highly lobulated nuclei of HGPS cells. This is in agreement with the finding that LAΔ50/progerin does not decrease Rb stability as is the case for LA containing a mutation in the Zmpste24 cleavage site (31). Therefore, the HGPS phenotype may not only be attributable to the abnormal farnesylation of LAΔ50/progerin, but also to the 50 aa that have been deleted near its C terminus.

Our observations also extend previous studies that link normal and accelerated aging to mitotic defects, including impaired chromosome segregation and increases in bi- and multinucleated cells (34, 35). With respect to the latter, we have found that some mitotic cells expressing high levels of LAΔ50/progerin show significant mitotic defects resulting in an even more delayed cytokinesis and in binucleated cells (SI Fig. 9 and SI Movie 5). This observation may help to explain the increased numbers of binucleated cells found in HGPS fibroblasts (see accompanying paper by Cao *et al.*; ref. 27).

Interestingly, it has been shown that low levels of LAΔ50/progerin mRNA and protein are expressed in normal cells derived from very young and old people (36) and that binucleated cells in normal populations react with an LAΔ50/progerin-specific antibody (see accompanying paper by Cao *et al.*). These results, along with the data presented in this study, indicate that the defects in cytokinesis, nuclear assembly, and progression through the cell cycle attributable to the expression of the mutant LA responsible for HGPS, may also contribute to normal human aging.

Materials and Methods

Cell Culture, Lamin Expression, and Synchronization. Dermal fibroblasts from progeria patients (HGADFN003 and HGADFN127; The Progeria Research Foundation Cell Bank, Peabody, MA) and from normal controls (AG08470 and AG09309; Coriell Cell Repositories, Camden, NJ) were grown as described in ref. 5. HeLa Tet-on cell lines stably transfected with plasmids encoding either GFP-myc-LA or GFP-myc-LAΔ50/progerin were maintained as described in ref. 19. Expression of GFP-fusion proteins was induced by the addition of 2 μg/ml doxycyclin to the growth medium for 24–50 h. For synchronizing HeLa Tet-on cells in mitosis, cells were incubated for 14 h in medium containing 0.2 μg/ml nocodazole. Inhibition of protein farnesylation was achieved by incubating cells in medium containing 5 μM FTI-277 (Calbiochem, San Diego, CA) for 50 h.

Preparation of Mitotic Cell Extracts. Mitotically arrested HeLa Tet-on cells expressing either GFP-myc-LA or GFP-myc-LAΔ50/progerin were harvested by mechanical shake-off, washed twice with PBS, incubated in ≈5 vol of ice-cold hypotonic buffer (10 mM Hepes, pH 7.4/10 mM NaCl/5 mM $MgCl_2$/2 mM EGTA/1 mM DTT/500 μg/ml DNase/200 μg/ml RNase) containing 1× Complete protease inhibitor mixture, EDTA-free (Roche, Basel, Switzerland), 20 μM cytochalasin B (Sigma, St. Louis, MO), phosphatase inhibitors [0.2 μM calyculin A (Calbiochem)/8 μM microcystin/0.5 mM β-glycerophosphate (both Sigma)] and homogenized in a glass–glass homogenizer. After the addition of 97 mM NaCl, the samples were incubated in the absence or presence of 1.6% Triton X-100 for 15 min on ice and supernatant and pellet fractions were collected by centrifugation for 20 min at 19,000 × *g*.

Characterization of Farnesylation and Carboxymethylation. HeLa Tet-on cells expressing GFP-myc-LAΔ50/progerin were incubated for 36 h with 30 μM AG, with or without FTI-277 (3 μM), in culture medium. Cells were lysed in RIPA buffer (PBS/1% Nonidet P-40/0.5% sodium deoxycholate/0.1% SDS/1 mM sodium orthovanadate/0.1 mg/ml PMSF/1:100 protease inhibitor cocktail solution) (Santa Cruz Biotechnology, Santa Cruz, CA), and GFP-LAΔ50/progerin was immunoprecipitated with anti-GFP [ab6556; Abcam (Cambridge, MA)] and analyzed by immunoblotting, using anti-AG (25) or anti-LA/C [clone 14; BD Biosciences (San Jose, CA)].

Carboxymethylation was determined essentially as described in ref. 12. HeLa cells expressing GFP-myc-LAΔ50/progerin were incubated with 50 μCi/ml ([*methyl*-^{3}H])methionine for 16–20 h and then lysed in RIPA buffer (Santa Cruz Biotechnology). Proteins were immunoprecipitated consecutively from the cell lysate with anti-LB (C-20; Santa Cruz Biotechnology), anti-LA/C (clone 14; BD Biosciences) or anti-GFP (AbCam, ab6556), separated by SDS/PAGE, and identified by immunoblotting with the appropriate antibodies. Protein bands were excised, incubated with 1 M KOH for 20 h in an Eppendorf (Boulder, CO) tube, and placed inside a scintillation vial containing scintillation mixture, and the diffusible counts were determined (base-releasable counts). The bands were then recovered and dissolved in perchloric acid-H_2O_2, and nonreleasable counts were determined by liquid scintillation. Relative methylation was calculated by using the following formula: Carboxymethylation % = ((Base

Releasable counts − Blank/Non-Base Releasable counts − Blank) × (no. methionines − 1)) × 100.

Immunofluorescence. Cells grown on cover slips were fixed either for 5 min at −20°C in methanol or for 15 min at room temperature in either 3% paraformaldehyde in PBS or 3.7% formaldehyde in PBS, followed by extraction in 0.1% Triton X-100 in PBS for 5 min at room temperature, and processed for immunofluorescence as described in ref. 19. Rabbit antibodies used were directed against LA [1:1,000; generated against a synthetic peptide with the sequence VTVTRSYRSVGGSG, which is not present in LAΔ50/progerin; PRB-113C (Covance, Princeton, NJ)], LB (1:200; ref. 9), phosphoRb(Ser-807/811) (1:100; Cell Signaling Technology, Danvers, MA) and cyclin D1 [1:200; H-295 (Santa Cruz Biotechnology)]; mouse monoclonal antibodies were directed against emerin [1:50; NCL-emerin (Novocastra, Newcastle, U.K.)] and Rb [1:100; 4H1 (Cell Signaling)]; rat anti-LA/C (1:1,200; no. 320, generated against bacterial expressed full-length human LA), and goat-anti LA/C [1:200; N-18 (Santa Cruz Biotechnology)]. The secondary antibodies used were anti-rabbit IgG-Alexa Fluor 488 and 568, anti-rat IgG-Alexa Fluor 488 or 568, anti-mouse IgG-Alexa Fluor 488 and 568, and anti-goat IgG-Alexa Fluor 568 (all 1:400; Molecular Probes). DNA was stained with Hoechst dye, and confocal images were taken with an LSM 510 META (Zeiss, Thornwood, NY).

Immunoblotting. Cell fractions were denatured in Laemmli buffer, separated by SDS/PAGE, and immunoblotted as described in ref. 5. Primary antibodies used were rat anti-LA/C (1:1,000; no. 270; ref. 5), rabbit anti-LB (1:1,200; ref. 9), rabbit anti-EGFP [1:5,000; ab6556 (AbCam)], mouse anti-AG (1:5,000; ref. 25), mouse anti-LA/C [1:5,000; clone 14 (BD Biosciences)], mouse anti-emerin [1:300; NCL-emerin (Novocastra)], and goat anti-LB [1:1,000; C-20 (Santa Cruz Biotechnology)]. Secondary antibodies were goat anti-rat IgG, anti-rabbit IgG, and anti-mouse IgG conjugated to horseradish peroxidase (all 1:1,000; Kirkegaard and Perry Laboratories, Gaithersburg, MD). Detection was achieved by using 4-chloro-1-naphtol/H_2O_2.

Statistical Analysis. A two-tailed homoscedastic Student's *t* test was used to compare mean levels. $P < 0.01$ was considered statistically significant.

This work was supported by the Kentucky Lung Cancer Research Program (D.A.A. and H.P.S.), the U.S. National Institute for General Medical Sciences (H.P.S.), a Schroedinger Fellowship from the Austrian Research Foundation (to T.D.), the U.S. National Cancer Institute, the U.S. National Institute on Aging, and the Ellison Foundation.

1. Hutchinson J (1886) *Medicochir Trans* 69:473–477.
2. Gilford M (1904) *Practitioner* 73:188–217.
3. De-Sandre-Giovannoli A, Bernard R, Cau P, Navarro C, Amiel J, Boccaccio I, Lyonnet S, Stewart CL, Munnich A, Le-Merrer M, Levy N (2003) *Science* 300:2055.
4. Eriksson M, Brown WT, Gordon LB, Glynn MW, Singer J, Scott L, Erdos MR, Robbins CM, Moses TY, Berglund P, *et al.* (2003) *Nature* 423:293–298.
5. Goldman RD, Shumaker DK, Erdos MR, Eriksson M, Goldman AE, Gordon LB, Gruenbaum Y, Khuon S, Mendez M, Varga R, Collins FS (2004) *Proc Natl Acad Sci USA* 101:8963–8968.
6. Mounkes LC, Stewart CL (2004) *Curr Opin Cell Biol* 16:322–327.
7. Ackerman J, Gilbert-Barness E (2002) *Pediatr Pathol Mol Med* 21:1–13.
8. Broers JL, Ramaekers FC, Bonne G, Yaou RB, Hutchison CJ (2006) *Physiol Rev* 86:967–1008.
9. Moir RD, Montag-Lowy M, Goldman RD (1994) *J Cell Biol* 125:1201–1212.
10. Goldman RD, Gruenbaum Y, Moir RD, Shumaker DK, Spann TP (2002) *Genes Dev* 16:533–547.
11. Kitten GT, Nigg EA (1991) *J Cell Biol* 113:13–23.
12. Sinensky M, Fantle K, Trujillo M, McLain T, Kupfer A, Dalton M (1994) *J Cell Sci* 107:61–67.
13. Bergo MO, Gavino B, Ross J, Schmidt WK, Hong C, Kendall LV, Mohr A, Meta M, Genant H, Jiang Y, *et al.* (2002) *Proc Natl Acad Sci USA* 99:13049–13054.
14. Corrigan DP, Kuszczak D, Rusinol AE, Thewke DP, Hrycyna CA, Michaelis S, Sinensky MS (2005) *Biochem J* 387:129–138.
15. Pendas AM, Zhou Z, Cadinanos J, Freije JM, Wang J, Hultenby K, Astudillo A, Wernerson A, Rodriguez F, Tryggvason K, Lopez-Otin C (2002) *Nat Genet* 31:94–99.
16. Rusinol AE, Sinensky MS (2006) *J Cell Sci* 119:3265–3272.
17. Liu B, Wang J, Chan KM, Tjia WM, Deng W, Guan X, Huang JD, Li KM, Chau PY, Chen DJ, *et al.* (2005) *Nat Med* 11:780–785.
18. Manju K, Muralikrishna B, Parnaik VK (2006) *J Cell Sci* 119:2704–2714.
19. Shumaker DK, Dechat T, Kohlmaier A, Adam SA, Bozovsky MR, Erdos MR, Eriksson M, Goldman AE, Khuon S, Collins FS, *et al.* (2006) *Proc Natl Acad Sci USA* 103:8703–8708.
20. Clements L, Manilal S, Love DR, Morris GE (2000) *Biochem Biophys Res Commun* 267:709–714.
21. Ozaki T, Saijo M, Murakami K, Enomoto H, Taya Y, Sakiyama S (1994) *Oncogene* 9:2649–2653.
22. Giacinti C, Giordano A (2006) *Oncogene* 25:5220–5227.
23. Zarkowska T, Mittnacht S (1997) *J Biol Chem* 272:12738–12746.
24. Parish CA, Rando RR (1996) *Biochemistry* 35:8473–8477.
25. Troutman JM, Roberts MJ, Andres DA, Spielmann HP (2005) *Bioconjug Chem* 16:1209–1217.
26. Dechat T, Vlcek S, Foisner R (2000) *J Struct Biol* 129:335–345.
27. Cao K, Capell BC, Erdos MR, Djabali K, Collins FS (2007) *Proc Natl Acad Sci USA* 104:4949–4954.
28. Tsai MY, Wang S, Heidinger JM, Shumaker DK, Adam SA, Goldman RD, Zheng Y (2006) *Science* 311:1887–1893.
29. Dechat T, Gajewski A, Korbei B, Gerlich D, Daigle N, Haraguchi T, Furukawa K, Ellenberg J, Foisner R (2004) *J Cell Sci* 117:6117–6128.
30. Kim WY, Sharpless NE (2006) *Cell* 127:265–275.
31. Nitta RT, Jameson SA, Kudlow BA, Conlan LA, Kennedy BK (2006) *Mol Cell Biol* 26:5360–5372.
32. Gotzmann J, Foisner R (2006) *Histochem Cell Biol* 125:33–41.
33. Varela I, Cadinanos J, Pendas AM, Gutierrez-Fernandez A, Folgueras AR, Sanchez LM, Zhou Z, Rodriguez FJ, Stewart CL, Vega JA, *et al.* (2005) *Nature* 437:564–568.
34. Baker DJ, Jeganathan KB, Cameron JD, Thompson M, Juneja S, Kopecka A, Kumar R, Jenkins RB, de Groen PC, Roche P, van Deursen JM (2004) *Nat Genet* 36:744–749.
35. Ly DH, Lockhart DJ, Lerner RA, Schultz PG (2000) *Science* 287:2486–2492.
36. Scaffidi P, Misteli T (2006) *Science* 312:1059–1063.